

The geology of SLGP is shown in Figure 2 (Leynes et al., 1996). The lithology is classified into 5 major stratigraphic units. The Cretaceous Ultramafics (CU) is the oldest rock unit mapped in the area. Exposures of this unit, which is made up of dark green to green, highly fractured serpentinites, are found in the southwest, near the Cabalian Bay. This unit is overlain unconformably by the buff to cream-colored and fossiliferous Tertiary Limestones (TL) on the southwest. Exposed in the western and northeastern portions of the area are sequences of clastic sedimentary rocks of conglomerates, turbidites, sandstones and calcisiltites capped by a thin but massive coral limestone deposits collectively referred to as the Tertiary Clastics (TC). Late Tertiary volcanic rocks (TV) are found in the north and western sector of Mt. Cabalian and are composed of moderately to highly altered basaltic andesite to andesite lava flows, as well as tuffs and tuff breccias intruded by microdiorite dikes. The Quaternary volcanics (QV) include the small strato-volcanoes such as Mts. Cantodoc and Cabalian, which are made up of alternating sequences of pyroclastic and lavas.

The main structures mapped in the area include two major splays of the Philippine fault, the Hindagan-Panian and Catmon-Bisay faults, delineated west and north-northwest of the study area. Several minor faults were also mapped in the area (Figures 1 & 2).

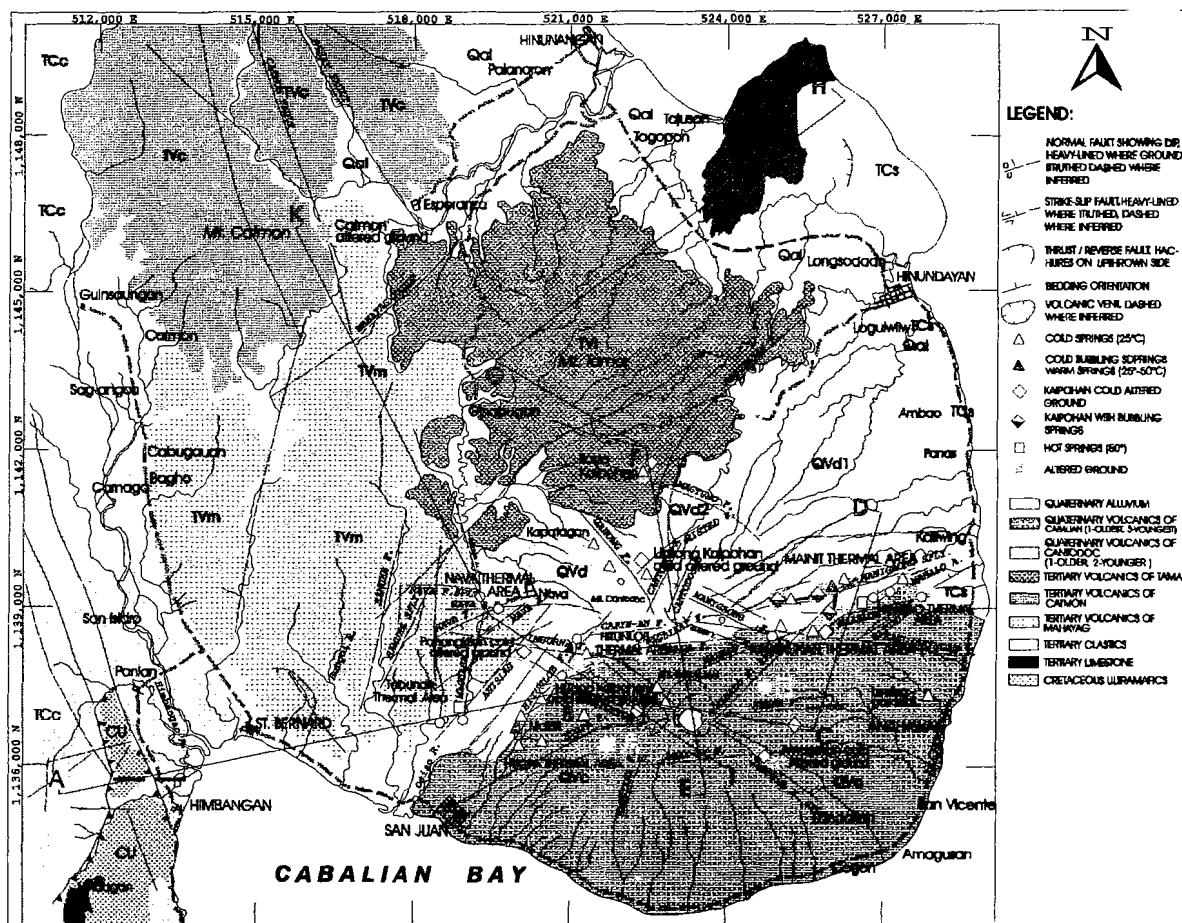


Figure 2. Geologic map of SLGP (from Leynes et al., 1996)

2.3 Geochemistry of thermal areas

Most of the thermal features such as hot and warm springs found in SLGP, are located at the eastern and western flanks of Mt. Cabalian (Figure 2). A unique thermal feature in SLGP is the presence of "kaipohans" or patches of ground characterized by intense acid alteration and high concentration of gases such as CO₂ and H₂S. In general, the spring waters of SLGP are classified into 3 groups: 1.) acid condensate, which are

composed mostly of dissolved gases like H_2S , i.e. Ilaya, 2.) mixed $Cl-HCO_3-SO_4$, which indicates significant deep hydrothermal components, i.e. Mainit, Mahalo and Tabun, and 3) dominantly HCO_3 , i.e. Nava, Hitunlob, Hugpa.

Analysis and plotting of these waters in a Na-K-Mg ternary diagram (Figure 3) reveal that all water samples group near the immature water region, forming a single dilution line which points to a source fluid temperature of $240^\circ C$. This also suggests that the thermal springs come from a single hydrothermal system (Leynes et al., 1996).

23 Geophysics

Resistivity surveys such as the DC Schlumberger resistivity traversing and vertical electrical sounding with a maximum AB/2 spacing of 1000 m, were conducted at SLGP as early as 1989 (Tebar et al., 1989). The resistivity surveys delineated two low resistivity zones (<20 R-m) situated on the eastern

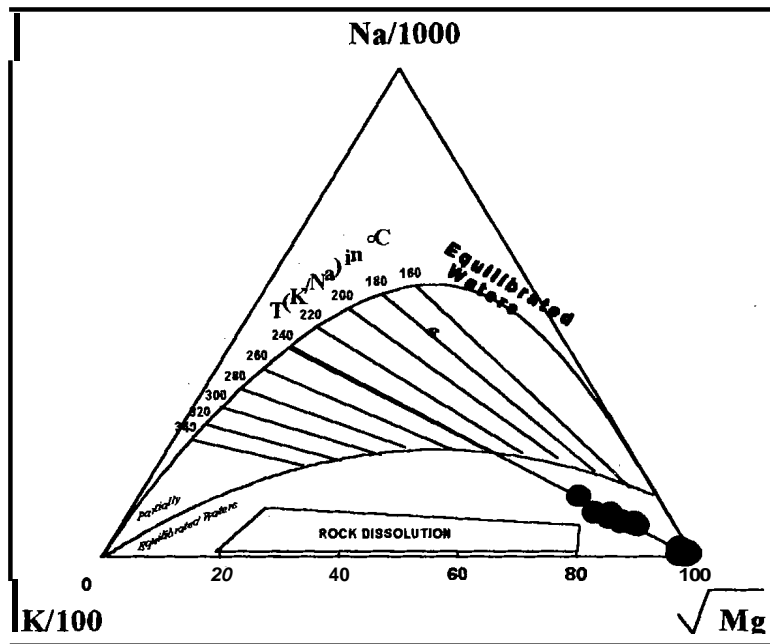


Figure 3. Na-K-Mg ternary plot of SLGP waters (Leynes et al., 1996); circle represents the water samples taken from the thermal areas.

(Mainit-Mahalo) and west-southwestern (Nava-Magcasa) flanks of Mt. Cabalian (Figure 4). These low resistivity zones are separated by a relatively high resistivity zone beneath Mts. Cabalian and Cantodoc. These low resistivity anomalies were postulated to be the outflow zones of an existing geothermal system centered beneath Mt. Cabalian. A gravity survey, carried out in mid-1996, revealed two gravity highs located directly beneath and northwest of Mt. Cabalian (Figure 5). These gravity highs were modeled to be shallow intrusives and interpreted to be the heat source of the existing geothermal system in the area (Catane and 3.

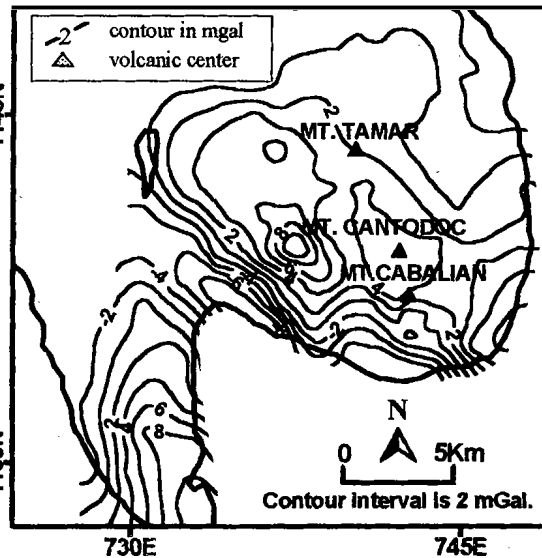
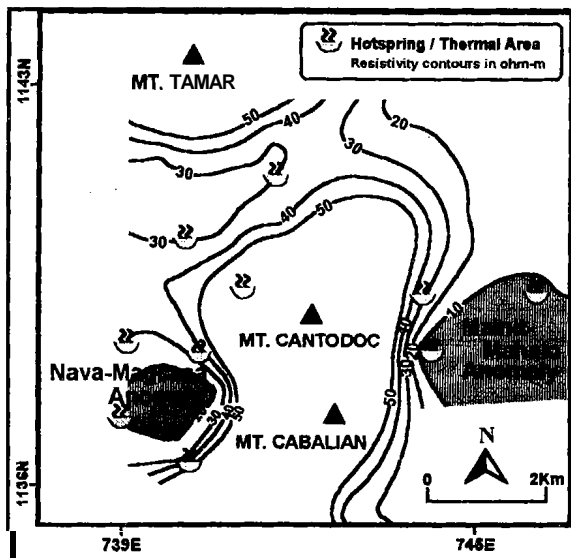


Figure 4. Apparent isoresistivity map at $AB/2=1000$ m (Tebar et al., 1989) Figure 5. Residual Bouguer anomaly map (Catane and Apuada, 1996)

MAGNETOTELLURIC(MT) SURVEY

A total of 39 MT stations (Figure 6) were measured using a Phoenix V-5 MT system which is capable of measuring frequencies in the range of 0.00055 to 384 Hz (Graham, 1991). Stations were spaced about 500 m to 1 km apart. All stations were oriented towards the magnetic north unless the ruggedness of the terrain did not permit it. The remote reference (RR) technique was applied during data acquisition for most sites.

In general, the quality of the MT data acquired was good for periods less than 1 s. Most signals at periods greater than 1s show scattering and large error bars. The determinant apparent resistivity and phase, which are invariant to rotation were used during 1-D inversion of the data. The impedance skews for most stations were low (<0.1), indicating little 3-dimensionality for the area. Rotation to the principal direction points to an angle of about -45° , which is consistent to the strike of the major faults found in the area (e.g. Catmon-Bisay fault zone).

31 Results

31.1 Inversion models

The SLGP MT data were processed using the MTTULK I-D inversion program. For each MT site, two inversions were performed. First, with few layers as possible (hereafter called 1-D layered models), and second, by Occam inversion, which fits the data by a "smooth" resistivity model. The Occam inversion not only minimizes the difference between the data and the model response but also minimizes the "roughness" (or maximizes the smoothness) of the model. There is a trade off between the model fit to the data and the roughness of the model, i.e. best fit to data gives rough models (Constable et al., 1987).

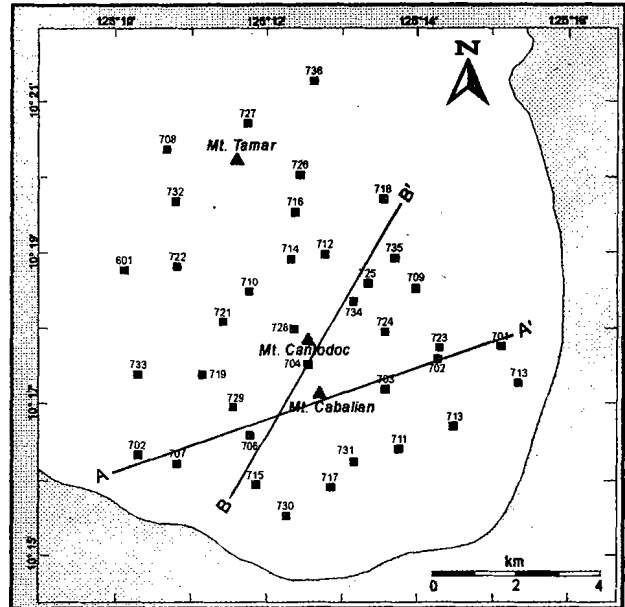


Figure 4 MT station location map (lines A-A' and B-B' are the profile lines used during modeling)

The general characteristic of the models from the 1-D inversion shows high surface resistivity ($>50 \Omega\text{-m}$), then low resistivity ($<10 \Omega\text{-m}$) at 100 to 2000 m depth, and then increasing resistivity ($>100 \Omega\text{-m}$) with depth.

31.2 Isoresistivity maps

The layered models derived from the smooth I-D Occam inversion were contoured in the form of isoresistivity maps at different depths.

The resistivity at 300 m depth in the survey area (Figure 7a); is less than $10 \Omega\text{-m}$ except for the area around Mts. Cabalian and Cantodoc, which is characterized by relatively high resistivity values of $>10 \Omega\text{-m}$. At 1000 m depth (Figure 7b), the broad low resistivity ($<10 \Omega\text{-m}$) anomaly is now divided into two, one in the northeastern and the other at the southern portion of Mt. Cabalian. The area bounded by the Mts. Cabalian and Cantodoc is enclosed by higher resistivity values ($>20 \Omega\text{-m}$). This high resistive region extends further to the west. However, it should be noted that the quality of the low frequency part of the data for sites near Mts. Cabalian and Cantodoc are poor, and therefore the results are not very reliable. At 2000 m depth (Figure 7c), the low resistivity anomaly on the northeast still exist, while the one on the south is greatly reduced and is shifted towards the western portion of Mt. Cabalian. The region beneath Mts. Cabalian and Cantodoc is still characterized by high resistivity values ($>20 \Omega\text{-m}$). At 5000 m depth (Figure 7d), the study area is now

bounded by resistivity values $>50 \Omega\text{-m}$ except for the anomaly zones in the northeast, where the resistivity is less than 20 R-m .

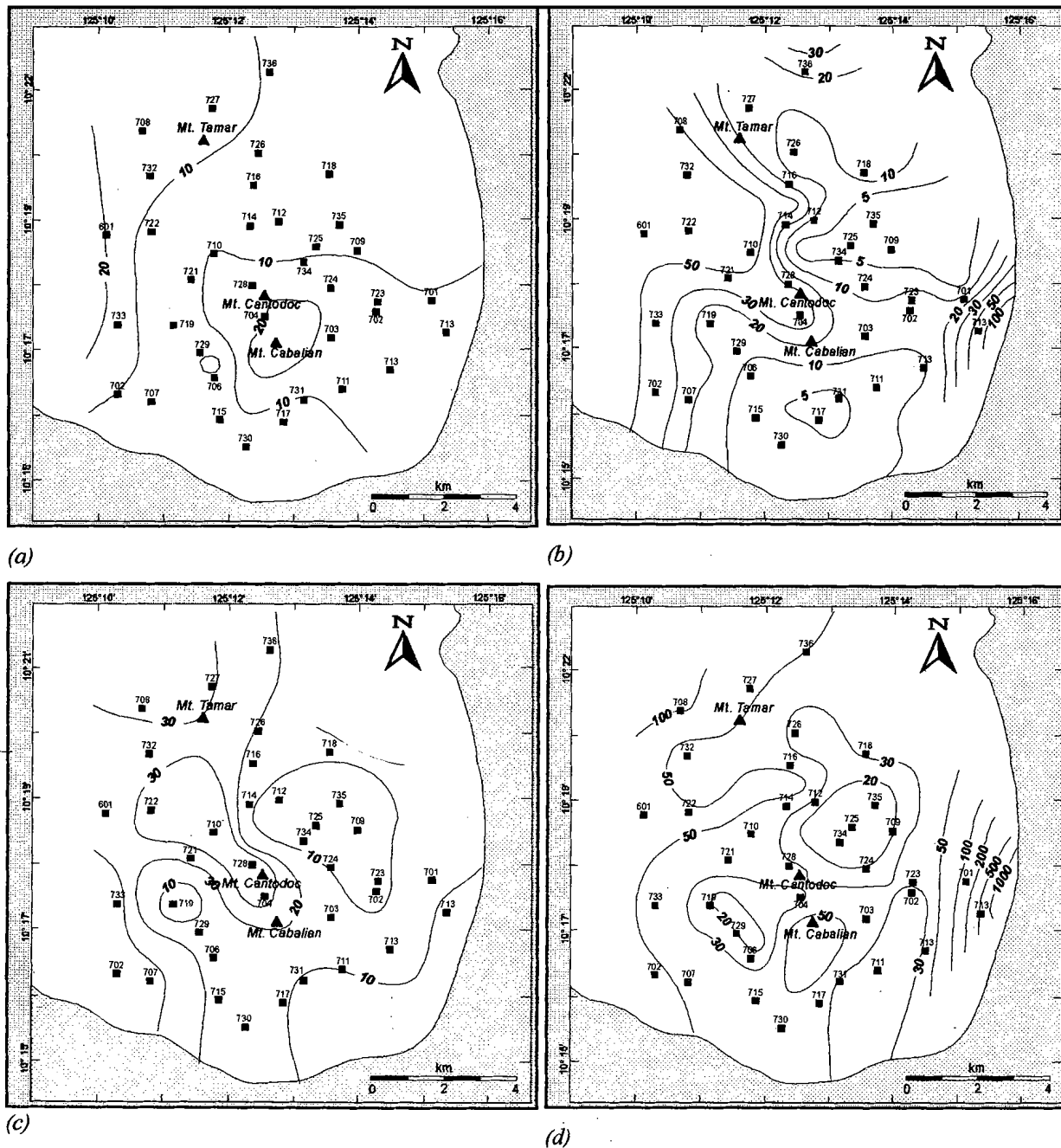


Figure 7. Isoresistivity maps at (a) 300 m, (b) 1000 m, (c) 2000 m, and (d) 5000 m depth; the contour lines are in $\Omega\text{-m}$.

3.1.3 Resistivity cross sections

Figure 8 shows the 1-D *Occam* model along the line A-A' (Figure 6) running WSW to ENE. A resistive layer caps the area down to depths of about 300 m. This is underlain by a thin (150 m) very low resistivity zone, which is found throughout the whole cross section except beneath the southwesternmost station (202). Further below is a broad less conductive region down to about 2500 m bsl with resistivity of 10-20 R-m, except in the

northeast where low resistivity is seen at around 1000-1500 m bsl. At greater depths, the resistivity increases. One conspicuous feature is the presence of a high resistivity zone ($>20 \Omega\text{-m}$) directly below Mt. Cabalian at about 500 to 1000 m depth.

A simplified cross-section along A-A' is shown on Figure 9 based on the 1-D layered inversion. It shows the same features, high resistivity at surface, a shallow conductive layer at depths of about 100 to 500 m and a broader conductive layer below it, which gets deeper towards the east. Further below, the resistivity increases with depth. Furthermore, this profile indicates that static shift is not a serious problem for this line. The broad low resistivity region at 1000-1500 m depth in the northeast which appeared in the Occam inversion (Figure 8), appears as a lower resistivity in the second layer beneath site 701.

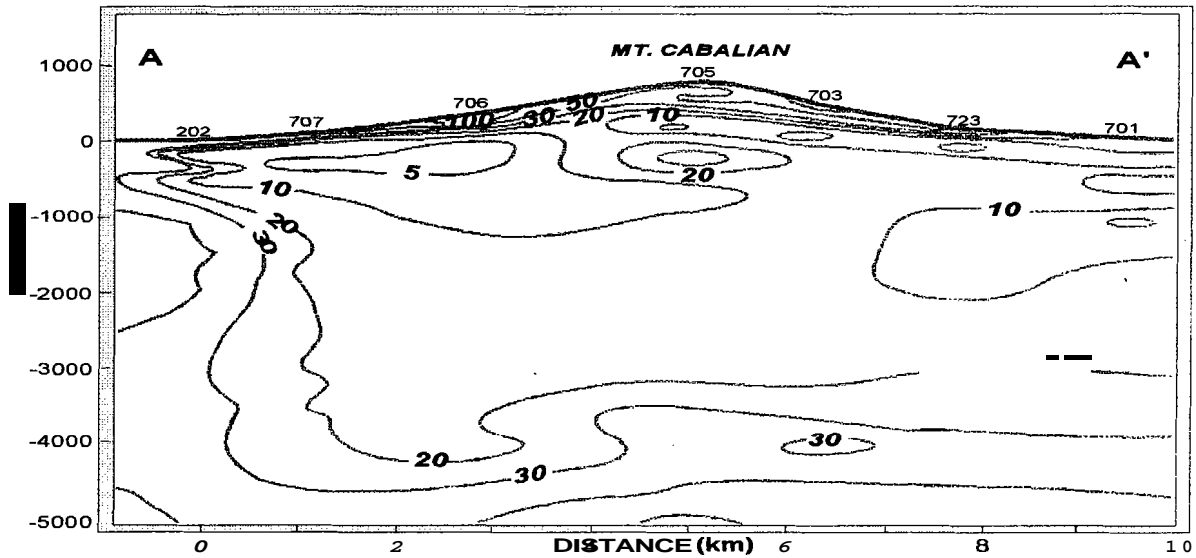
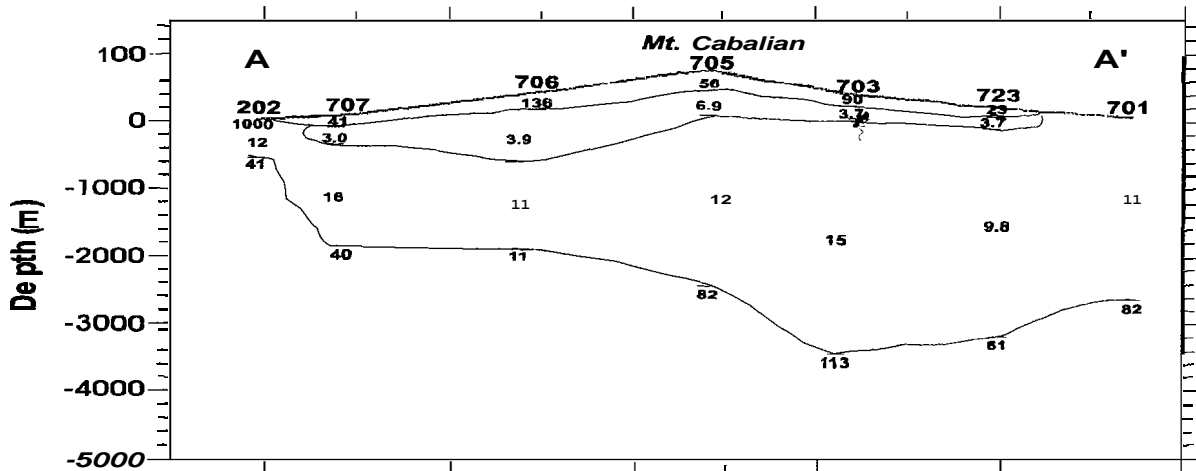


Figure 8. 1-D Occam model along line A-A'; contour lines are in $\Omega\text{-m}$.



resistivity of $<5 \Omega\text{-m}$, 2) in the northern part, also at 300-500 m depth with resistivity less than $5 \Omega\text{-m}$ and 3), at 1000-2500 m depth also with resistivity of $<5 \Omega\text{-m}$. A relatively high resistive block is detected below the volcanoes starting at a depth of 500 m.

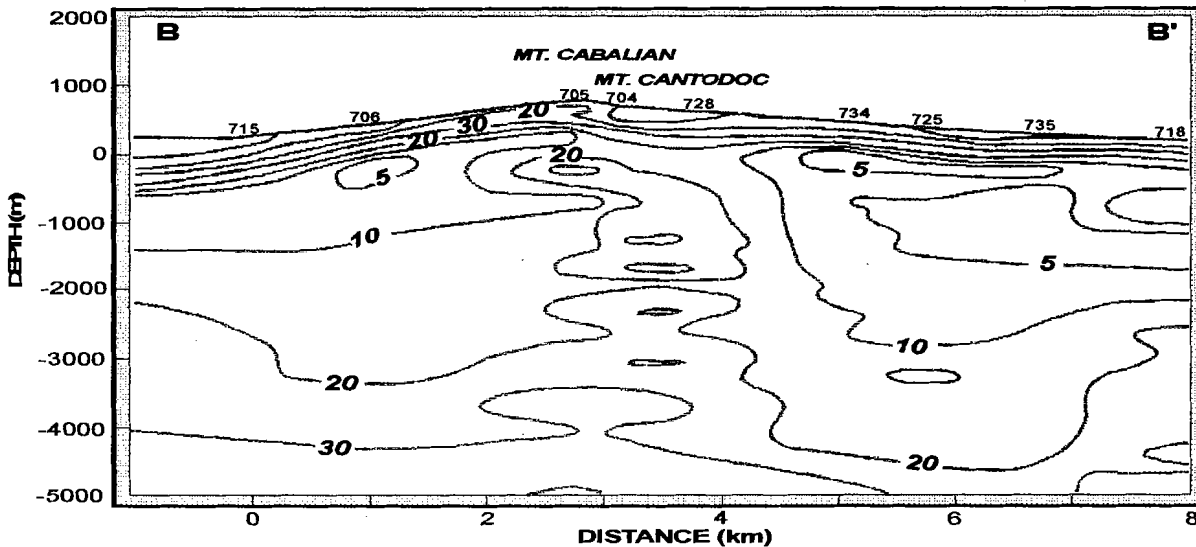
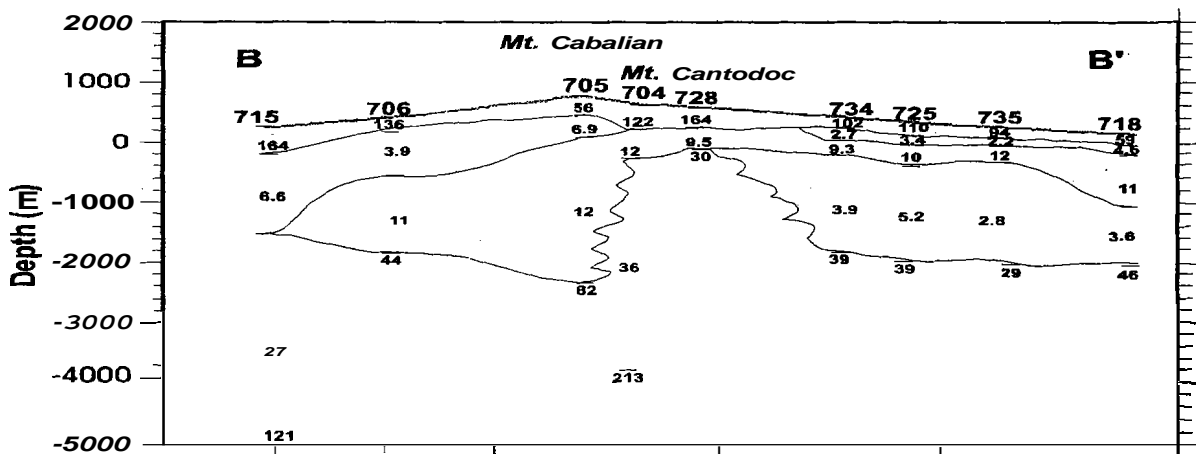


Figure 10. I-D Occam model along line B-B'; contour lines are in $\Omega\text{-m}$.

Similar resistivity structure is found by the 1-D layered inversion, shown in Figure 11. The same layers are observed by using the I-D layered models (Figure 11). A resistive cap rock exists at the surface down to 200 m depth. This is underlain by one to three conductive layers ($<12 \text{ R-m}$) down to about 2000 m bsl. In the southwest, the resistivity is $<10 \text{ S-m}$ in the first low resistivity layer down to 500 to 1500 m bsl and becomes shallower towards Mt. Cabalian. Below is a 12-16 R-m layer down to depths of 2000 m bsl, where the resistivity increases again. In the northeastern part, three low resistivity layers are detected. The first is a thin, highly conductive layer ($<5 \Omega\text{-m}$) at 100 to 200 m bsl. The second conductor has slightly higher resistivity ($10 \Omega\text{-m}$) than the first conductor and is found at 200 to 500 m bsl. This layer extends to the southwest. The third conductor has resistivity of $<5 \text{ R-m}$ at 500 to 2000 m bsl. Below, the resistivity increases. There is a relatively resistive body ($>30 \Omega\text{-m}$) beneath Mts. Cabalian and Cantodoc starting at depths of 500 m bsl.



4. CONCLUSION

The MT method mapped two low resistivity anomalies: one located on the **W-SW** of Mt. Cabalian and the other on the NE of the same volcano. **Similar** low resistivity anomalies were **mapped by** the DC Schlumberger **surveys** but their depth extent **was** not delineated due to the shallow penetration depth of the method. The anomaly on the **northeast** extends at greater **depths (as deep as 3000 m)** than the SW anomaly and is more conductive. The **area** is **capped by** a resistive layer that can be associated with the young volcanic deposits of the Quaternary volcanoes of Mts. **Cabalian** and **Cantodoc**. **A localized high** resistivity zone **occurs** beneath the volcanoes, which can be correlated to the shallow intrusive **body** modeled **by** the gravity **survey**. Highly resistive layers are seen at greater depths.

ACKNOWLEDGEMENTS

I wish to thank Dr. Ingvar B. Fridleifsson and Mr. Ludvik S. Georgsson for giving me the opportunity to participate in the UNU Geothermal Training Programme, where this report was prepared as my Diploma Project. I also would like to express my gratitude to Dr. Hjalmar Eysteinnsson, my adviser, for sharing his expertise in MT processing and interpretation. Thanks is also due to the UNU lecturers for unselfishly teaching us about the other **aspects** of geothermal energy. My appreciation also goes to **Ms.** Gudrun Bjarnadottir and the other UNU fellows, for making my stay in Iceland **as** comfortable as possible. Lastly, I also would like to extend my sincere gratitude for the **support** given to me **by** my colleagues at PNOC-EDC.

REFERENCES

Catane, J. P. L. And Apuada, N. A., 1996: A gravity investigation of the Southern Leyte Geothermal Prospect. **Proceedings from** the 18th PNOC-EDC annual geothermal conference, 288-295

Constable, S. C., Parker, R. L., Constable, C. G., 1987: **Occam s** inversion: A practical algorithm for generating smooth models from electromagnetic sounding **data**. Geophysics, Vol. 52, No. 3, 289-300

Datuin, R. T., 1982: **An** insight on Quaternary volcanoes and volcanic rocks of the Philippines. Journal of the Geological Society of the Philippines, Vol. 36, No. 1, 1-11

Gough, D. I. and Ingham, M. R., 1983: Interpretation methods for magnetometer arrays. Reviews of Geophysics and **Space** Physics, Vol. 21, No.4, 805-827.

Graham, G. B., 1991: Overview of Phoenix V-5 MT receiver, 8 pp.

Leynes, R. D., Bayon, F. E. B. and Camit, G. R. A., 1996: The geology and geochemistry of the Southern Leyte Geothermal Project. **Proceedings from** the 18th PNOC-EDC **annual** geothermal conference, 13-21

Patra, H. P. and Mallick, K. 1980: Geosounding principles, 2 Time-varying geoelectric **soundings**. Elsevier Scientific Publishing Company, Amsterdam, The Netherlands. 419 pp.

Swift, C. M., Jr., 1967: A magnetotelluric investigation of **an** electrical conductivity anomaly in the southwestern United States: Ph. D. thesis, Mass. Inst. Of tech.

Tebar, H. J., Pagado, E. S., Villarosa, H. G. A., Buenviaje, M. M., Vergara, M.C., Maneja, F. C., Catane, J. P. L., and Herras, E. B., 1989. Geoscientific exploration and evaluation of the Mt. Cabalian Geothermal Prospect, Southern Leyte. Unpublished PNOC EDC internal report, 77 pp.